ResearchGate

See discussions, stats, and author profiles for this publication at: https://www.researchgate.net/publication/324811987

Bedrock Erosion Surfaces Record Former East Antarctic Ice Sheet Extent

Article *in* Geophysical Research Letters · April 2018

DOI: 10.1029/2018GL077268

CITATION
1

READS
91

9 authors, including:

Michael Bentley
Durham University
158 PUBLICATIONS **4,131** CITATIONS
SEE PROFILE

Egidio Armadillo
Università degli Studi di Genova
68 PUBLICATIONS **300** CITATIONS
SEE PROFILE

German Leitchenkov
The All-Russia Scientific Research Institute for Geology and Mineral Resources of the …
93 PUBLICATIONS **1,444** CITATIONS
SEE PROFILE

Some of the authors of this publication are also working on these related projects:

Project Tectonics of the East Antarctic Margin View project

Project Antarctic Subglacial Topography and Ice Sheet Interactions View project

All content following this page was uploaded by German Leitchenkov on 31 May 2018.

The user has requested enhancement of the downloaded file.

AGU100 ADVANCING EARTH AND SPACE SCIENCE

Geophysical Research Letters

RESEARCH LETTER
10.1029/2018GL077268

Key Points:
- We report the discovery of plateau-like erosion surfaces within the Wilkes Subglacial Basin in East Antarctica
- Geomorphology and elevation of the plateaus are consistent with an early ice margin situated >400–500 km inland for extended periods
- If future major ice sheet retreat into the basin occurs, isostatic rebound will enable the plateaus to act as seeding points for ice rises

Supporting Information:
- Supporting Information S1
- Data Set S1

Correspondence to:
G. J. G. Paxman,
guy.j.paxman@durham.ac.uk

Citation:
Paxman, G. J. G., Jamieson, S. S. R., Ferraccioli, F., Bentley, M. J., Ross, N., Armadillo, E., et al. (2018). Bedrock erosion surfaces record former East Antarctic Ice Sheet extent. *Geophysical Research Letters*, *45*, 4114–4123. https://doi.org/10.1029/2018GL077268

Received 26 JAN 2018
Accepted 14 APR 2018
Accepted article online 27 APR 2018
Published online 9 MAY 2018

©2018. The Authors.
This is an open access article under the terms of the Creative Commons Attribution License, which permits use, distribution and reproduction in any medium, provided the original work is properly cited.

Bedrock Erosion Surfaces Record Former East Antarctic Ice Sheet Extent

Guy J. G. Paxman[1], Stewart S. R. Jamieson[1], Fausto Ferraccioli[2], Michael J. Bentley[1], Neil Ross[3], Egidio Armadillo[4], Edward G. W. Gasson[5], German Leitchenkov[6,7], and Robert M. DeConto[8]

[1]Department of Geography, Durham University, Durham, UK, [2]British Antarctic Survey, Cambridge, UK, [3]School of Geography, Politics and Sociology, Newcastle University, Newcastle Upon Tyne, UK, [4]Dipartimento di Scienze della Terra, dell'Ambiente e della Vita, Università di Genova, Genoa, Italy, [5]Department of Geography, Sheffield University, Sheffield, UK, [6]Institute for Geology and Mineral Resources of the World Ocean, St. Petersburg, Russia, [7]Institute of Earth Sciences, St. Petersburg State University, St. Petersburg, Russia, [8]Department of Geosciences, University of Massachusetts, Amherst, MA, USA

Abstract East Antarctica hosts large subglacial basins into which the East Antarctic Ice Sheet (EAIS) likely retreated during past warmer climates. However, the extent of retreat remains poorly constrained, making quantifying past and predicted future contributions to global sea level rise from these marine basins challenging. Geomorphological analysis and flexural modeling within the Wilkes Subglacial Basin are used to reconstruct the ice margin during warm intervals of the Oligocene-Miocene. Flat-lying bedrock plateaus are indicative of an ice sheet margin positioned >400–500 km inland of the modern grounding zone for extended periods of the Oligocene-Miocene, equivalent to a 2-m rise in global sea level. Our findings imply that if major EAIS retreat occurs in the future, isostatic rebound will enable the plateau surfaces to act as seeding points for extensive ice rises, thus limiting extensive ice margin retreat of the scale seen during the early EAIS.

Plain Language Summary The Wilkes Subglacial Basin is a large, low-lying topographic depression situated beneath the Antarctic Ice Sheet. Because the land surface of the basin is currently situated below sea level, it is a potential site of ice sheet collapse and rapid retreat in a warming world. Understanding this landscape and how it has evolved through time in relation to past climate and sea level is therefore key to understanding the future dynamics of this part of the ice sheet. Here we report the discovery, using ice-penetrating radar data sets, of extensive subglacial bedrock plateaus within the Wilkes Subglacial Basin. We analyze the geomorphology of these plateau surfaces and reconstruct the evolution of the subglacial landscape through time. Our results indicate that this part of the Wilkes Subglacial Basin was free of ice for extensive and prolonged periods of time during the early stages of ice sheet development. These constraints on past ice sheet extent, together with our landscape reconstruction, can be used by the ice sheet modeling community to better understand the likely future dynamics of this part of the Antarctic Ice Sheet.

1. Introduction

Ice thickness measurements from ice-penetrating radar surveys show that ~40% of the Antarctic Ice Sheet (AIS) is marine-based (Fretwell et al., 2013). This includes not only much of the West Antarctic Ice Sheet (WAIS) but also large subglacial basins around the margin of the East Antarctic Ice Sheet (EAIS). These low-lying subglacial basins are thought to be vulnerable to rapid ice sheet retreat in response to ocean and climate warming (DeConto & Pollard, 2016; Li et al., 2015; Mercer, 1978; Pollard et al., 2015; Schoof, 2007). Loss of all marine-based ice in East Antarctica would raise global mean sea level by ~20 m (Fretwell et al., 2013). However, there is currently no consensus regarding the amount of ice sheet retreat during past warmer climates (DeConto & Pollard, 2016) and consequent uncertainty as to the likely magnitude and rate of future retreat of the EAIS into these marine-based subglacial basins.

The Wilkes Subglacial Basin (WSB) has attracted attention as a potential area of substantial ice sheet retreat because the EAIS is grounded >500 m below sea level across much of the 1,400-km-long × 200 to 600-km-wide basin (Fretwell et al., 2013; Mengel & Levermann, 2014; Figure 1). However, significant variation remains between numerical ice sheet model predictions of EAIS retreat within the WSB during past warmer periods such as the mid-Pliocene (ca. 3 Ma) and mid-Miocene (ca. 14 Ma; Austermann et al., 2015; DeConto &

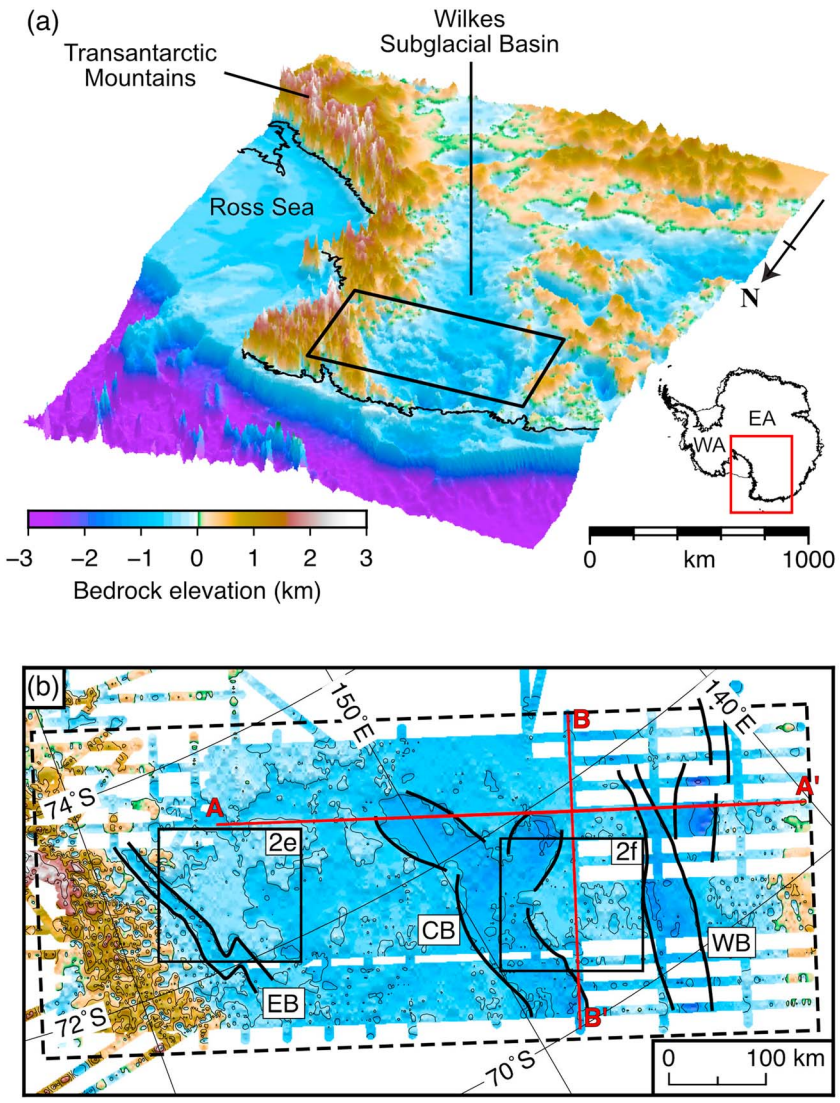

Figure 1. Regional setting of the Wilkes Subglacial Basin in East Antarctica. (a) Perspective image of the regional bedrock topography (Fretwell et al., 2013). Bedrock elevations have not been isostatically adjusted for ice sheet loading. Vertical exaggeration = 150x. The black box shows the extent of panel b. The inset shows the study region within East Antarctica. (b) Bedrock topography of the main survey grid (Ferraccioli et al., 2009). The black lines show basin margins (Ferraccioli et al., 2009; Jordan et al., 2010). The red lines and the solid boxes show locations of profiles and panels in Figure 2. The dashed box marks the outline of the main survey grid. Abbreviations: EA = East Antarctica; WA = West Antarctica; CB = Central Basin; EB = Eastern Basin; WB = Western Basin.

Pollard, 2016; Mengel & Levermann, 2014; Pollard et al., 2015). Moreover, despite attempts to elucidate the likely stability of the EAIS within the WSB from geological, geomorphological, and oceanographic evidence (Barrett, 2013; Cook et al., 2013; Gasson, DeConto, & Pollard, 2016; Sugden et al., 1995), the location, amount, and rate of ice sheet retreat within the WSB during warmer climates such as the Pliocene remain poorly understood.

An important but largely untapped record of the stability of the EAIS is the morphology of the bedrock topography within the WSB. Subglacial geomorphology, as unveiled by airborne radar surveys, has been used to infer the configuration, basal thermal regime, and marginal zone locations of past and present ice sheets (Jamieson et al., 2014). For example, ice-penetrating radar has revealed subglacial landforms and areas of enhanced glacial erosion indicative of former ice margins within the Aurora Subglacial Basin (Aitken et al., 2016; Young et al., 2011). We analyze airborne radar data to investigate the subglacial landscape within the WSB and assess its relationship with past EAIS dynamics. Combining geomorphological interpretation and flexural modeling, we constrain the ice sheet extent during warm intervals in the early stages of EAIS

development in Oligocene-early Miocene times and identify how the bedrock topography could influence the future dynamics of this part of the ice sheet.

2. Data and Methods

In the 2005/2006 austral summer, a UK-Italian airborne geophysical survey acquired >60,000 line-km of radio-echo sounding data across the northern part of the WSB (Ferraccioli et al., 2009; Jordan et al., 2010, 2013; Figures 1, S1, and S2 in the supporting information). We subtracted the radar-derived ice thickness from the ice surface elevation for each radar line in order to determine the bedrock elevation. A digital elevation model of the northern WSB (Figure 1) was produced by interpolating the bedrock elevation line data onto a 1-km grid (Wessel et al., 2013). We computed the hypsometry (elevation-frequency distribution), along-track roughness of the radar-derived topography (Shepard et al., 2001), and bedrock slope in order to characterize the subglacial landscape (supporting information).

We used 3-D flexural models to reconstruct the elevation of the northern WSB since EAIS inception at ca. 34 Ma. We isostatically adjusted the bedrock topography for the removal of the modern ice load (supporting information). Redistribution of surface material by erosion and sedimentation also induces a flexural response from the lithosphere that drives vertical surface displacement. The net amount of glacial erosion across the basin was estimated by assuming that flat-lying bedrock topographic highs are remnants of a formerly continuous pre-erosion surface, which is reconstructed by interpolation between these topographic highs (supporting information; Champagnac et al., 2007; Stern et al., 2005). We estimated the distribution of eroded material by subtracting the observed topography from this "peak accordance surface" (Figure S5). The seismically mapped distribution of offshore post-34 Ma sediment was used to determine the flexural response to sediment loading and to constrain our erosion estimate by comparing the mass of sediment to the mass of eroded material (Figure S6).

We computed the flexural response to erosional unloading and sediment loading using a 3-D model of a thin elastic plate overlying an inviscid fluid mantle (Watts, 2001). We assumed mean densities of 2,500 kg m^{-3} for eroded rock and 2,000 kg m^{-3} for offshore sediment and a uniform effective elastic thickness of 35 km (Wilson et al., 2012; supporting information). Eroded bedrock was restored to the topography, which was also adjusted for the associated flexural effects, producing a reconstruction of bedrock elevation at ca. 34 Ma. Using offshore sediment cores (Escutia et al., 2011; Tauxe et al., 2012), we established a chronology of glacial erosion and flexural uplift from 34 Ma to present (supporting information). This allowed us to produce paleo-elevation reconstructions at three important time slices associated with EAIS development: (1) the Eocene-Oligocene Boundary (ca. 34 Ma), (2) the mid-Miocene Climatic Optimum (ca. 14 Ma), and (3) the mid-Pliocene warm period (ca. 3 Ma).

Evolving dynamic topography (i.e., surface displacement by mantle dynamics) may have affected regional bedrock elevations during the Oligocene-Neogene. However, the magnitude of these changes is still poorly known, and hence, we do not incorporate them. We note, however, that dynamic topography models predict that during the mid-Pliocene the bedrock elevation was ~100–200 m lower on the western and northern margins of the WSB (Austermann et al., 2015).

3. Results

3.1. Bedrock Topography and Geomorphology

The radar data image extensive flat bedrock surfaces within the northern WSB. We identify these plateau-like surfaces (Figure 2) by their remarkably constant elevation, bright reflectivity, small-scale surface roughness, and steep edges. The new digital elevation model (Figure 1) reveals that the plateau surfaces are laterally continuous over tens to hundreds of kilometers (~30% of the survey grid) but are not observed in exploratory radar survey lines located to the north or south (Figures S1 and S3). The flat surfaces are separated by a complex network of subbasins up to 80 km wide, wherein the ice sheet bed lies up to 2.1 km below sea level (Ferraccioli et al., 2009; Figure 1). Three major subbasins are defined: the Eastern, Central, and Western Basins (Ferraccioli et al., 2009; Figure 1).

The elevations of the flat plateau-like surfaces are broadly uniform across the basin, with a modal elevation of 560 m below sea level (Figure 2). If the topography is isostatically rebounded for the removal of the present-

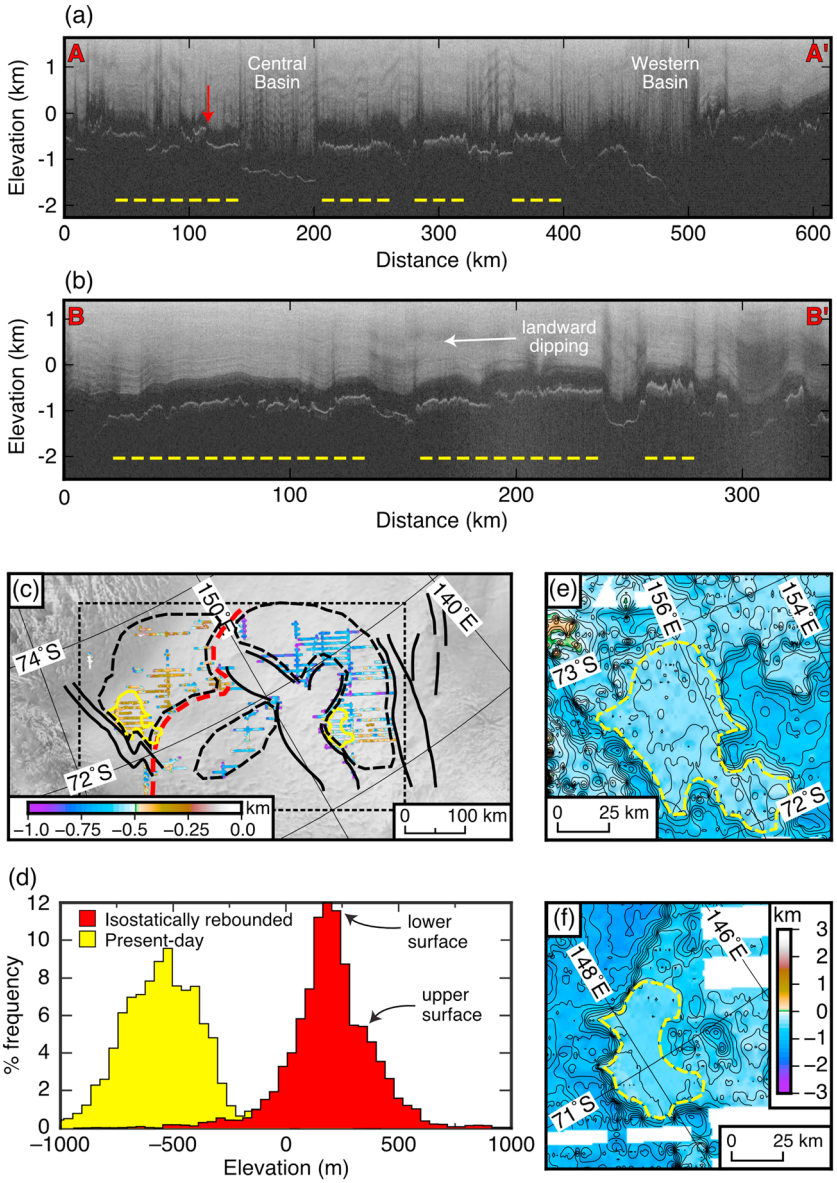

Figure 2. Flat-topped plateau surfaces within the Wilkes Subglacial Basin (WSB). (a) Radar echogram along profile A-A′ crossing the flat plateau surfaces. Profile is oriented E-W, and ice flow is out of the page. (b) Profile B-B′ running S-N along an extensive plateau surface showing a gentle landward dip. Profile locations shown in Figure 1b. The dashed yellow lines highlight the horizontal extent of the plateau surfaces. The red arrow marks the break in slope between surfaces. (c) Location of plateau surfaces, colored according to the present-day elevation of subglacial topography. The dashed red line shows the break in slope. The black lines show subbasin outlines (Ferraccioli et al., 2009). The black dashed lines mark the extent of the plateau surface remnants. The dashed box indicates the area shown in Figure 3. (d) Histogram of plateau surface elevations (hypsometry), expressed as a % frequency of the total flat surface area. Yellow = present-day elevation; red = elevation isostatically adjusted for removal of the present-day ice load. Hypsometric peaks corresponding to the upper and lower plateau surfaces are indicated. (e) Map of part of the upper plateau surface in the eastern WSB. (f) Map of part of the lower plateau surface in the western WSB. The contour interval is 100 m. The dashed yellow outlines show particularly flat and smooth areas of the plateau surface (also shown in panel c).

day ice sheet, the modal plateau surface elevation is 200 m above sea level. When rebounded for ice loading, the plateaus are remarkably flat-lying over their entire extent; the hypsometric curve is unimodal, with a standard deviation of ~150 m (Figure 2). The only clear tilt observed on the surfaces is a gentle inland (north to south) dip of 0.1° (Figure 2c), attributed to inland thickening of the ice sheet. The plateaus are incised by small-scale valleys, with local relief of ~100 m (Figures 2a and 2b). Some areas of the plateau surfaces have a very low slope (<1°), minor basal roughness, and no evidence of incision (Figure S4). Our mapping reveals two plateau levels, separated by an ~200-m break of slope or escarpment (Figure 2). The

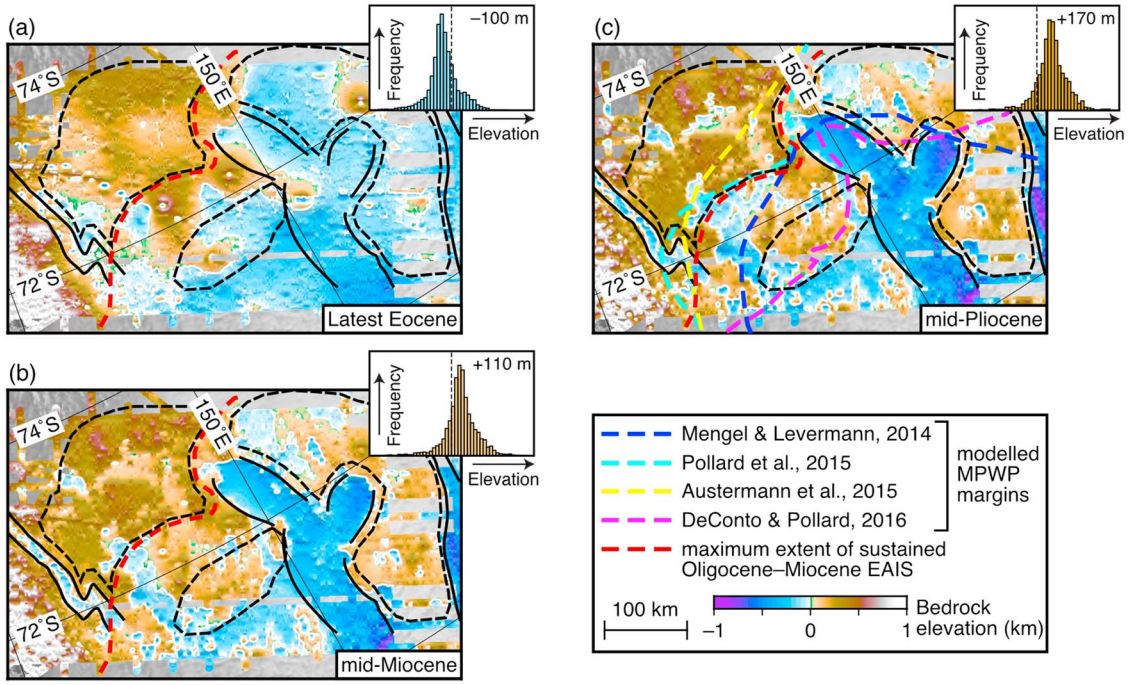

Figure 3. Bedrock elevation reconstruction. (a) Latest Eocene, immediately prior to East Antarctic Ice Sheet (EAIS) inception at the Eocene-Oligocene boundary (34 Ma). Plateau surface remnants are shown by the dashed outlines. The red dashed line marks the escarpment at the limit of the remnants of the lower plateau surface, which constrains the maximum extent of the EAIS margin during sustained and extended periods of the Oligocene-Miocene. (b) Mid-Miocene (14 Ma). The subbasins (solid lines) have been glacially overdeepened by a dynamic and fluctuating EAIS. (c) Mid-Pliocene (3 Ma). The colored dashed lines show modeled mid-Pliocene warm period ice margins (Austermann et al., 2015; DeConto & Pollard, 2016; Mengel & Levermann, 2014; Pollard et al., 2015). The white lines denote the sea level (0 m) contour. The insets show the hypsometry of the plateau surfaces at each time interval. The quoted values denote the modal plateau surface elevation relative to present-day sea level (vertical dashed line).

plateau surface remnants south of the break of slope are rougher and ~200 m higher than the remnants north of the break of slope (Figure S4).

3.2. Flexural Modeling

Our erosion estimate shows that >1 km of material has been selectively eroded from the overdeepened subbasins within the WSB since the latest Eocene. Removal of this material has driven 200–300 m of flexural uplift of the plateau surfaces between these subbasins (Figure S5). We estimated a total eroded mass of ~6×10^5 Gt, which compares well with the observed mass of post-34 Ma WSB-derived detrital sediment on the Wilkes Land margin of ~$7–9 \times 10^5$ Gt (supporting information).

Our flexural models show that at the Eocene-Oligocene Boundary, the plateau surface remnants below the break of slope restore to a modal elevation of −100 m (Figure 3). By the mid-Miocene, these surface remnants had been flexurally uplifted above sea level and were situated at a modal elevation of 110 m (Figure 3). During the mid-Pliocene, the plateaus were 170 m above sea level when free of ice cover (Figure 3), although this is likely an overestimate due to potential dynamic uplift since the mid-Pliocene (Austermann et al., 2015). When free of ice cover, the remnants of the plateau surface below the escarpment were within ±100 m of sea level between the Oligocene and early Miocene, whereas the surface above the escarpment (when ice free) has remained above sea level since 34 Ma (Figure S7 and Table S1 in the supporting information).

4. Discussion

4.1. Mechanism of Plateau Surface Formation

The plateaus identified in the WSB resemble subglacial bedrock erosion surfaces previously mapped along the Siple Coast (Wilson & Luyendyk, 2006) and the Weddell Sea Embayment (Rose et al., 2015; Figure S8). Planation surfaces (the Crohn erosion surface) are also exposed in the Prince Charles Mountains in the

Lambert Glacier region, >1 km above sea level (Wellman & Tingey, 1981; White, 2013). Three reasons lead us to propose that the WSB plateaus are also the remnants of a once continuous erosion surface, rather than depositional topographic features. First, glacial sedimentary deposition predominates at the ice sheet margin, whereas the plateau surfaces are 300–500 km inland of the modern margin. Second, interpretations of aeromagnetic anomalies suggest that this area of the WSB comprises Devonian-Triassic Beacon Supergroup rocks and intrusive Ferrar dolerites (Ferraccioli et al., 2009) and does not contain thick Cenozoic sedimentary deposits (Ferraccioli et al., 2009; Jordan et al., 2013). Third, the small-scale roughness of the surfaces, as observed in radar echograms, is consistent with valley incision into a bedrock surface, as opposed to the smoother topography of depositional sediment-filled subglacial basins (Bingham & Siegert, 2009).

One possible explanation for plateau surface formation is that the WSB was characterized by long-lived low-lying coastal plains immediately prior to and during the early stages of EAIS development. The plateau remnants we have mapped and reconstructed in the WSB are analogous to the low-elevation Nullarbor Plain and Murray Basin planation surfaces along the conjugate South Australian passive margin, which are inferred to have formed during Eocene-Miocene times (Quigley et al., 2010; Sandiford et al., 2009). These planation surfaces cover a horizontal extent of hundreds of km, are situated <200 m above sea level, and bounded at the inland margin by 100 to 200 m-high escarpments, which are interpreted as marking Miocene paleo-shorelines (Quigley et al., 2010). These observations are directly comparable to the lower-level WSB planation surface, implying a similar timing and mode of formation.

Alternatively, the lower WSB planation surface may have formed by fluvial and hillslope processes and/or wave action at sea level in front of a retreating escarpment following Gondwana breakup, analogous to Gondwanan passive margins such as eastern Australia and southern Africa (Beaumont et al., 2000; Jamieson & Sugden, 2008; Sugden & Denton, 2004). However, these passive margins exhibit escarpments >1,000 m in elevation, compared to the 200-m escarpment in the WSB. Moreover, apatite fission track data from the Wilkes Land coast show ages of >250 Ma, implying very little erosion along the margin since the Triassic, which is inconsistent with major escarpment retreat concomitant with Gondwana breakup in the Late Cretaceous (Arne et al., 1993).

A final possibility is that the plateaus are remnants of a much older terrestrial erosion surface formed prior to Gondwana breakup. However, potential field models indicate that the subbasins of the WSB are superimposed on pre-existing fault systems, which were likely active during Cretaceous-early Cenozoic upper crustal extension and/or transtension at the margin of the East Antarctic Craton (Cianfarra & Salvini, 2016; Ferraccioli et al., 2009). If the plateaus were older than Cretaceous-early Cenozoic, we would expect to observe faulting and high-angle tilting of the plateau blocks, as is recognized in association with the West Antarctic Rift System (LeMasurier & Landis, 1996). Moreover, flexure associated with TAM uplift (occurring episodically through the mid Cretaceous to Paleogene; Fitzgerald, 2002; Lisker & Läufer, 2013) would also be expected to induce subtle tilting of the plateau surfaces (Jordan et al., 2013). As such systematic tilts are not observed (Figure S4), our preferred interpretation is that the surface planation continued after faulting and flexure.

The model that best fits the observed morphology and paleo-elevation reconstructions of the planation surface remnants within the WSB is one in which surface planation began close to sea level following Gondwana breakup, Cretaceous-early Cenozoic transtension, and TAM uplift (i.e., since the Eocene). We propose that low-lying vegetated coastal plains, shallow inland seas, and/or brackish marshes likely dominated the landscape of the northern WSB shortly prior to and during the early stages of EAIS development (Figure 4). Given the large horizontal extent (~300 km) of the plateaus, a protracted period of time (millions to tens of millions of years) would be required for surface planation by fluvial processes. This implies that surface planation was analogous to the South Australian passive margin and likely occurred from the Eocene onward and during the Oligocene-early Miocene, at which time the plateaus were situated at elevations within 100 m of sea level (Figure 3).

4.2. Past East Antarctic Ice Sheet Behavior and Extent

Our combined geomorphological and flexural modeling analysis indicates that the WSB plateau surfaces were situated close to sea level in Oligocene-early Miocene times. Near-coastal surface planation in the absence of ice during the Oligocene-early Miocene would have required a restricted ice sheet for

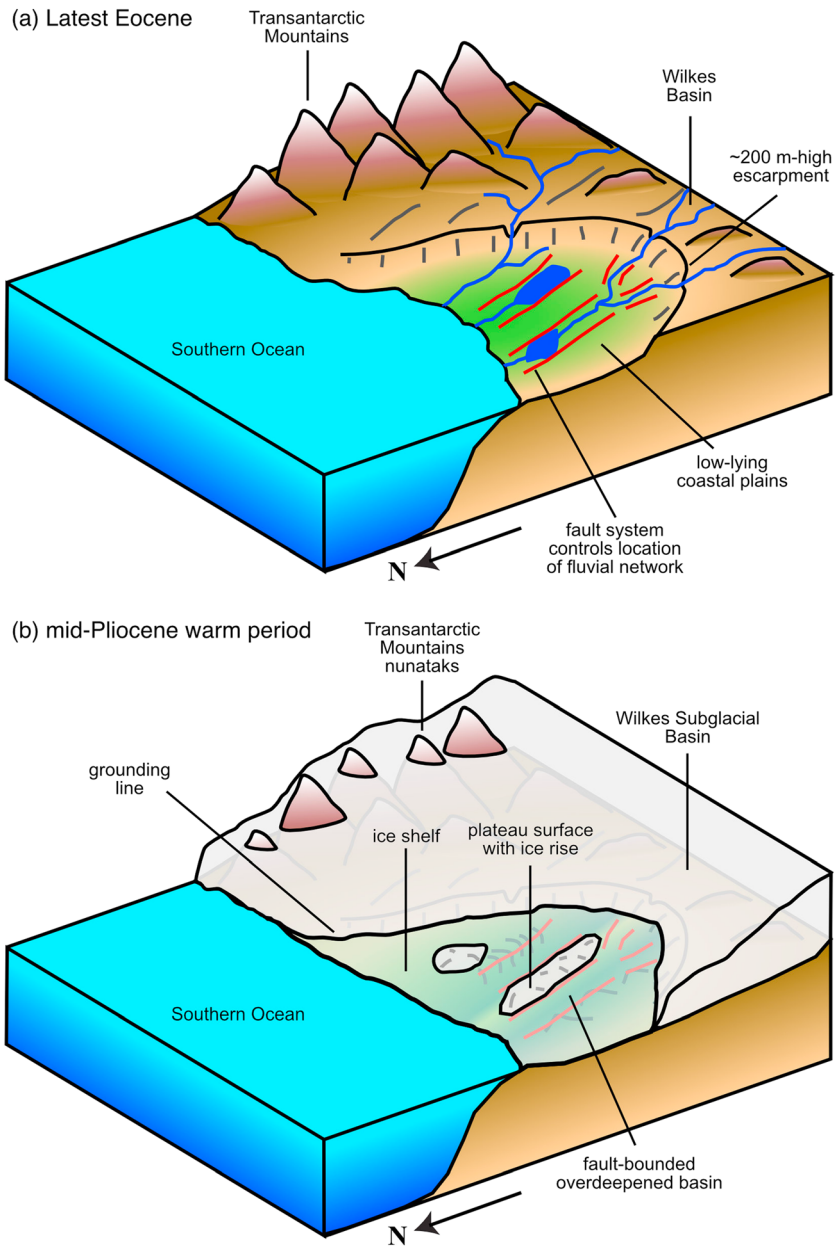

Figure 4. Schematic landscape and ice sheet configurations within the Wilkes Subglacial Basin. (a) An ice-free late Eocene (immediately prior to East Antarctic Ice Sheet [EAIS] inception at 34 Ma) landscape, characterized by low-elevation coastal plains hosting continental river systems. The EAIS margin was situated inland of the coastal plains for sustained periods during Oligocene-Miocene times. (b) Mid-Pliocene warm period (or potential future) ice sheet. Ice sheet retreat into the WSB is steered along the fault-bounded subbasins that have been selectively eroded by dynamic ice sheets. Ice rises are grounded on the plateaus that represent remnants of the coastal planation surfaces. These ice rises may slow further retreat of the margin.

extended periods during this time, with a terrestrial margin >400–500 km inland of the modern grounding line (Figure 4). Retreat of the ice sheet margin from the modern grounding line to this restricted configuration would be associated with a global sea level rise of >2 m from the WSB alone. A restricted and dynamic Oligocene-Miocene AIS is also evidenced by marine oxygen isotope and sea level records (Miller, 2005; Zachos et al., 2001) and recent ice sheet model simulations (Gasson, DeConto, Pollard, et al., 2016).

Wilkes Land offshore sediment records indicate that the majority of the volume of glacially eroded terrigenous material was removed by erosion prior to and/or during the expansion of the EAIS at ca. 14 Ma (supporting information; Escutia et al., 2011; Pierce et al., 2017; Tauxe et al., 2012). A slowdown in source-area erosion

rates at ca. 14 Ma is also indicated by detrital thermochronology and markers of erosion-driven isostatic uplift in the Lambert Glacier catchment to the west (Hambrey et al., 2007; Hambrey & McKelvey, 2000; Paxman et al., 2016; Thomson et al., 2013; Tochilin et al., 2012). Glacial erosion was focused within the relict WSB subbasins (Figure S5). The scale of these basins, alongside potential field modeling, implies that they are superimposed on pre-existing tectonic features (Aitken et al., 2014; Ferraccioli et al., 2009; Jordan et al., 2013). These subbasins were likely overdeepened beneath dynamic ice sheets that expanded over the northern WSB during cooler periods during the Oligocene-Neogene (Jamieson et al., 2010; Mengel & Levermann, 2014; Pierce et al., 2017) and exploited the pre-existing topographic depressions.

Because this fjord-and-plateau landscape would have required millions of years to form, we assert that the ice margin resided >400–500 km inland of its modern location for prolonged periods of time from the late Eocene to mid-Miocene and periodically advanced and retreated across the northern WSB. The plateaus have likely been subsequently preserved beneath non-erosive cold-based ice, while enhanced glacial flow and incision are focused in adjacent tectonically controlled topographic depressions (Sugden & John, 1976). The similarity between the elevation and extent of the WSB plateaus and those observed along the Siple Coast (Wilson & Luyendyk, 2006) and Weddell Sea Embayment (Rose et al., 2015) (Figure S8) is indicative of similar dynamic ice sheet behavior in West Antarctica and East Antarctica, at least up to Miocene times.

4.3. Plateau Surface Influence on Ice Sheet Dynamics

After formation in the Eocene-Miocene, the flat surfaces may have played a role in subsequent EAIS behavior. The present-day Siple Dome, Engelhardt, and Berkner Island ice rises are grounded on extensive shallow seabed plateaus (Paxman et al., 2017; Wilson & Luyendyk, 2006) akin to those we have described within the WSB, and the lateral extent and bedrock elevation of these ice rises are also comparable (Matsuoka et al., 2015; Figure S8). Our flexural models show that the plateau surfaces were close to sea level when free of significant ice cover (Figure 3), which would facilitate ice rise formation. Furthermore, the plateaus have been flexurally uplifted due to glacial erosion since 34 Ma (Figure 3), which suggests that ice rise formation has become more likely over time. We propose that the WSB plateau-like surfaces hosted extensive ice rises within an ice shelf during interglacial periods when the EAIS retreated into the WSB and the plateaus were unloaded and isostatically uplifted (Figure 4).

The plateaus lie along the southern margin of the predicted retreated region of the EAIS in numerical simulations for the mid-Pliocene warm period (Austermann et al., 2015; DeConto & Pollard, 2016; Mengel & Levermann, 2014; Pollard et al., 2015; Figure 3). Numerical models indicate that the presence of ice rises inhibits ice margin retreat through an increased buttressing effect (Favier & Pattyn, 2015; Matsuoka et al., 2015). These plateau surfaces may therefore have slowed EAIS retreat during recent interglacials such as the mid-Pliocene and also formed important nucleation points for ice sheet regrowth during glacial periods, although the rate of bedrock rebound following deglaciation may have been relatively slow owing to the high viscosity of the mantle beneath East Antarctica (Whitehouse et al., 2012). This provides a potential analogue for future ice sheet response in a warming world; if the EAIS were to retreat into the WSB in the future, isostatic rebound would enable the plateau surfaces to act as seeding points for ice rises, thus potentially delaying further retreat of the EAIS and/or facilitating a temporary readvance of the ice sheet margin (Matsuoka et al., 2015).

5. Conclusions

We conclude that the newly mapped bedrock plateau surfaces within the WSB provide (a) a constraint on the extent of the EAIS during Oligocene-Miocene warm intervals and (b) an improved understanding of the processes that likely operated at the ice sheet margin during subsequent retreat phases and may operate in the future. Plateau surface formation by fluvial erosion requires an ice sheet margin situated >400–500 km inland of the modern grounding zone during prolonged periods of the Oligocene-Miocene. These near-sea level plateaus likely facilitated ice rise formation when exposed during subsequent warm interglacials, potentially buttressing the margin against further retreat (Matsuoka et al., 2015). The glacial dynamics associated with the plateau surfaces may therefore exert considerable influence over EAIS behavior (Favier & Pattyn, 2015; Gudmundsson, 2013). Improving numerical models to incorporate feedbacks related to these bedrock topographic features may significantly influence predictions of future ice sheet retreat and contribute to our understanding of the overall long-term stability of this part of the EAIS.

Acknowledgments

We thank everyone involved with the planning and implementation of the WISE-ISODYN airborne geophysical survey. We wish to thank Tom Jordan for providing the radar echograms and Pippa Whitehouse for helpful sea level discussions. We also thank Stuart Thomson for his constructive review, which greatly improved the final manuscript. G.J.G.P. was supported by the Natural Environment Research Council UK studentship NE/L002590/1. G.L. acknowledges Russian Science Foundation grant 16-17-10139. The processed WISE-ISODYN radar data are freely available on the NERC/BAS Polar Data Centre airborne geophysics data portal (https://doi.org/10.5285/59e5a6f5-e67d-4a05-99af-30f656569401). Modern-day and reconstructed topography grids produced as part of this study are available to download in the supporting information. This paper is dedicated to the memory of Graham Paxman.

References

Aitken, A. R. A., Roberts, J. L., van Ommen, T. D., Young, D. A., Golledge, N. R., Greenbaum, J. S., et al. (2016). Repeated large-scale retreat and advance of Totten Glacier indicated by inland bed erosion. *Nature*, *533*(7603), 385–389. https://doi.org/10.1038/nature17447

Aitken, A. R. A., Young, D. A., Ferraccioli, F., Betts, P. G., Greenbaum, J. S., Richter, T. G., et al. (2014). The subglacial geology of Wilkes Land, East Antarctica. *Geophysical Research Letters*, *41*, 2390–2400. https://doi.org/10.1002/2013GL058954

Arne, D. C., Kelly, P. R., Brown, R. W., & Gleadow, A. J. W. (1993). Reconnaissance apatite fission-track data from the East Antarctic Shield. In R. H. Findlay, et al. (Eds.), *Gondwana Eight: Assembly, evolution and dispersal* (pp. 605–611). Hobart: Balkema.

Austermann, J., Pollard, D., Mitrovica, J. X., Moucha, R., Forte, A. M., DeConto, R. M., et al. (2015). The impact of dynamic topography change on Antarctic ice sheet stability during the mid-Pliocene warm period. *Geology*, *43*(10), 927–930. https://doi.org/10.1130/G36988.1

Barrett, P. J. (2013). Resolving views on Antarctic Neogene glacial history—The Sirius debate. *Earth and Environmental Science Transactions of the Royal Society of Edinburgh*, *104*(1), 31–53. https://doi.org/10.1017/S175569101300008X

Beaumont, C., Kooi, H., & Willett, S. (2000). Coupled tectonic-surface process models with applications to rifted margins and collisional orogens. In M. A. Summerfield (Ed.), *Geomorphology and global tectonics* (pp. 29–55). Chichester: Wiley.

Bingham, R. G., & Siegert, M. J. (2009). Quantifying subglacial bed roughness in Antarctica: Implications for ice-sheet dynamics and history. *Quaternary Science Reviews*, *28*(3–4), 223–236. https://doi.org/10.1016/j.quascirev.2008.10.014

Champagnac, J. D., Molnar, P., Anderson, R. S., Sue, C., & Delacou, B. (2007). Quaternary erosion-induced isostatic rebound in the western Alps. *Geology*, *35*(3), 195–198. https://doi.org/10.1130/G23053A.1

Cianfarra, P., & Salvini, F. (2016). Origin of the Adventure Subglacial Trench linked to Cenozoic extension in the East Antarctic Craton. *Tectonophysics*, *670*, 30–37. https://doi.org/10.1016/j.tecto.2015.12.011

Cook, C. P., Van De Flierdt, T., Williams, T., Hemming, S. R., Iwai, M., Kobayashi, M., et al. (2013). Dynamic behaviour of the East Antarctic Ice Sheet during Pliocene warmth. *Nature Geoscience*, *6*(9), 765–769. https://doi.org/10.1038/ngeo1889

DeConto, R. M., & Pollard, D. (2016). Contribution of Antarctica to past and future sea-level rise. *Nature*, *531*(7596), 591–597. https://doi.org/10.1038/nature17145

Escutia, C., Brinkhuis, H., & Klaus, A. (2011). IODP expedition 318: From greenhouse to icehouse at the Wilkes Land Antarctic Margin. *Scientific Drilling*, *12*, 15–23. https://doi.org/10.2204/iodp.sd.12.02.2011

Favier, L., & Pattyn, F. (2015). Antarctic ice rise formation, evolution, and stability. *Geophysical Research Letters*, *42*, 4456–4463. https://doi.org/10.1002/2015GL064195

Ferraccioli, F., Armadillo, E., Jordan, T., Bozzo, E., & Corr, H. (2009). Aeromagnetic exploration over the East Antarctic Ice Sheet: A new view of the Wilkes Subglacial Basin. *Tectonophysics*, *478*(1–2), 62–77. https://doi.org/10.1016/j.tecto.2009.03.013

Fitzgerald, P. G. (2002). Tectonics and landscape evolution of the Antarctic plate since the breakup of Gondwana, with an emphasis on the West Antarctic Rift System and the Transantarctic Mountains. *Royal Society of New Zealand Bulletin*, *35*, 453–469.

Fretwell, P., Pritchard, H. D., Vaughan, D. G., Bamber, J. L., Barrand, N. E., Bell, R., et al. (2013). Bedmap2: Improved ice bed, surface and thickness datasets for Antarctica. *The Cryosphere*, *7*(1), 375–393. https://doi.org/10.5194/tc-7-375-2013

Gasson, E., DeConto, R. M., & Pollard, D. (2016). Modeling the oxygen isotope composition of the Antarctic ice sheet and its significance to Pliocene Sea level. *Geology*, *44*(10), 827–830. https://doi.org/10.1130/G38104.1

Gasson, E., DeConto, R. M., Pollard, D., & Levy, R. H. (2016). Dynamic Antarctic ice sheet during the early to mid-Miocene. *Proceedings of the National Academy of Sciences of the United States of America*, *113*(13), 3459–3464. https://doi.org/10.1073/pnas.1516130113

Gudmundsson, G. H. (2013). Ice-shelf buttressing and the stability of marine ice sheets. *The Cryosphere*, *7*(2), 647–655. https://doi.org/10.5194/tc-7-647-2013

Hambrey, M. J., Glasser, N., Mckelvey, B., Sugden, D., & Fink, D. (2007). Cenozoic landscape evolution of an East Antarctic oasis (Radok Lake area, northern Prince Charles Mountains), and its implications for the glacial and climatic history of Antarctica. *Quaternary Science Reviews*, *26*(5–6), 598–626. https://doi.org/10.1016/j.quascirev.2006.11.014

Hambrey, M. J., & McKelvey, B. (2000). Major Neogene fluctuations of the East Antarctic Ice Sheet: Stratigraphic evidence from the Lambert Glacier region. *Geology*, *28*(10), 887–890. https://doi.org/10.1130/0091-7613(2000)28<887:MNFOTE>2.0.CO;2

Jamieson, S. S. R., Stokes, C. R., Ross, N., Rippin, D. M., Bingham, R. G., Wilson, D. S., et al. (2014). The glacial geomorphology of the Antarctic ice sheet bed. *Antarctic Science*, *26*(6), 724–741. https://doi.org/10.1017/S0954102014000212

Jamieson, S. S. R., & Sugden, D. E. (2008). Landscape evolution of Antarctica. In A. K. Cooper, et al. (Eds.), *Antarctica: A keystone in a changing world* (pp. 39–54). Washington, DC: The National Academies Press. https://doi.org/10.1007/s13398-014-0173-7.2

Jamieson, S. S. R., Sugden, D. E., & Hulton, N. R. J. (2010). The evolution of the subglacial landscape of Antarctica. *Earth and Planetary Science Letters*, *293*(1–2), 1–27. https://doi.org/10.1016/j.epsl.2010.02.012

Jordan, T. A., Ferraccioli, F., Armadillo, E., & Bozzo, E. (2013). Crustal architecture of the Wilkes Subglacial Basin in East Antarctica, as revealed from airborne gravity data. *Tectonophysics*, *585*, 196–206. https://doi.org/10.1016/j.tecto.2012.06.041

Jordan, T. A., Ferraccioli, F., Corr, H., Graham, A., Armadillo, E., & Bozzo, E. (2010). Hypothesis for mega-outburst flooding from a palaeo-subglacial lake beneath the East Antarctic Ice Sheet. *Terra Nova*, *22*(4), 283–289. https://doi.org/10.1111/j.1365-3121.2010.00944.x

LeMasurier, W. E., & Landis, C. A. (1996). Mantle-plume activity recorded by low-relief erosion surfaces in West Antarctica and New Zealand. *Bulletin of the Geological Society of America*, *108*(11), 1450–1466. https://doi.org/10.1130/0016-7606(1996)108<1450:MPARBL>2.3.CO;2

Li, X., Rignot, E., Morlighem, M., Mouginot, J., & Scheuchl, B. (2015). Grounding line retreat of Totten Glacier, East Antarctica, 1996 to 2013. *Geophysical Research Letters*, *42*(19), 8049–8056. https://doi.org/10.1002/2015GL065701

Lisker, F., & Läufer, A. L. (2013). The Mesozoic Victoria Basin: Vanished link between Antarctica and Australia. *Geology*, *41*(10), 1043–1046. https://doi.org/10.1130/G33409.1

Matsuoka, K., Hindmarsh, R. C. A., Moholdt, G., Bentley, M. J., Pritchard, H. D., Brown, J., et al. (2015). Antarctic ice rises and rumples: Their properties and significance for ice-sheet dynamics and evolution. *Earth-Science Reviews*, *150*, 724–745. https://doi.org/10.1016/j.earscirev.2015.09.004

Mengel, M., & Levermann, A. (2014). Ice plug prevents irreversible discharge from East Antarctica. *Nature Climate Change*, *4*(6), 451–455. https://doi.org/10.1038/nclimate2226

Mercer, J. H. (1978). West Antarctic ice sheet and CO2 greenhouse effect: A threat of disaster. *Nature*, *104*(25), 10,335–10,339. https://doi.org/10.1073/pnas.0703993104

Miller, K. G. (2005). The Phanerozoic record of global sea-level change. *Science*, *310*(5752), 1293–1298. https://doi.org/10.1126/science.1116412

Paxman, G. J. G., Jamieson, S. S. R., Ferraccioli, F., Bentley, M. J., Forsberg, R., Ross, N., et al. (2017). Uplift and tilting of the Shackleton Range in East Antarctica driven by glacial erosion and normal faulting. *Journal of Geophysical Research: Solid Earth*, *122*, 2390–2408. https://doi.org/10.1002/2016JB013841

Paxman, G. J. G., Watts, A. B., Ferraccioli, F., Jordan, T. A., Bell, R. E., Jamieson, S. S. R., & Finn, C. A. (2016). Erosion-driven uplift in the Gamburtsev Subglacial Mountains of East Antarctica. *Earth and Planetary Science Letters*, *452*, 1–14. https://doi.org/10.1016/j.epsl.2016.07.040

Pierce, E. L., van de Flierdt, T., Williams, T., Hemming, S. R., Cook, C. P., & Passchier, S. (2017). Evidence for a dynamic East Antarctic Ice Sheet during the mid-Miocene climate transition. *Earth and Planetary Science Letters*, *478*, 1–13. https://doi.org/10.1016/j.epsl.2017.08.011

Pollard, D., DeConto, R. M., & Alley, R. B. (2015). Potential Antarctic Ice Sheet retreat driven by hydrofracturing and ice cliff failure. *Earth and Planetary Science Letters*, *412*, 112–121. https://doi.org/10.1016/j.epsl.2014.12.035

Quigley, M. C., Clark, D., & Sandiford, M. (2010). Tectonic geomorphology of Australia. *Geological Society, London, Special Publications*, *346*(1), 243–265. https://doi.org/10.1144/SP346.13

Rose, K. C., Ross, N., Jordan, T. A., Bingham, R. G., Corr, H. F. J., Ferraccioli, F., et al. (2015). Ancient pre-glacial erosion surfaces preserved beneath the West Antarctic Ice Sheet. *Earth Surface Dynamics*, *3*(1), 139–152. https://doi.org/10.5194/esurf-3-139-2015

Sandiford, M., Quigley, M., de Broekert, P., & Jakica, S. (2009). Tectonic framework for the Cenozoic cratonic basins of Australia. *Australian Journal of Earth Sciences*, *56*(sup1), S5–S18. https://doi.org/10.1080/08120090902870764

Schoof, C. (2007). Ice sheet grounding line dynamics: Steady states, stability, and hysteresis. *Journal of Geophysical Research*, *112*, F03S28. https://doi.org/10.1029/2006JF000664

Shepard, M. K., Campbell, B. A., Bulmer, M. H., Farr, T. G., Gaddis, L. R., & Plaut, J. J. (2001). The roughness of natural terrain: A planetary and remote sensing perspective. *Journal of Geophysical Research*, *106*(E12), 32,777–32,795. https://doi.org/10.1029/2000JE001429

Stern, T. A., Baxter, A. K., & Barrett, P. J. (2005). Isostatic rebound due to glacial erosion within the Transantarctic Mountains. *Geology*, *33*(3), 221–224. https://doi.org/10.1130/G21068.1

Sugden, D. E., & Denton, G. H. (2004). Cenozoic landscape evolution of the Convoy Range to Mackay Glacier area, Transantarctic Mountains: Onshore to offshore synthesis. *Geological Society of America Bulletin*, *116*(7), 840–857. https://doi.org/10.1130/B25356.1

Sugden, D. E., Denton, G. H., & Marchant, D. R. (1995). Landscape evolution of the Dry Valleys, Transantarctic Mountains: Tectonic implications. *Journal of Geophysical Research*, *100*(B6), 9949–9968. https://doi.org/10.1029/94JB02875

Sugden, D. E., & John, B. S. (1976). *Glaciers and landscape*. London: Edward Arnold.

Tauxe, L., Stickley, C. E., Sugisaki, S., Bijl, P. K., Bohaty, S. M., Brinkhuis, H., et al. (2012). Chronostratigraphic framework for the IODP expedition 318 cores from the Wilkes Land margin: Constraints for paleoceanographic reconstruction. *Paleoceanography*, *27*, PA2214. https://doi.org/10.1029/2012PA002308

Thomson, S. N., Reiners, P. W., Hemming, S. R., & Gehrels, G. E. (2013). The contribution of glacial erosion to shaping the hidden landscape of East Antarctica. *Nature Geoscience*, *6*(3), 203–207. https://doi.org/10.1038/ngeo1722

Tochilin, C. J., Reiners, P. W., Thomson, S. N., Gehrels, G. E., Hemming, S. R., & Pierce, E. L. (2012). Erosional history of the Prydz Bay sector of East Antarctica from detrital apatite and zircon geo- and thermochronology multidating. *Geochemistry, Geophysics, Geosystems*, *13*, Q11015. https://doi.org/10.1029/2012GC004364

Watts, A. B. (2001). *Isostasy and flexure of the lithosphere*. Cambridge: Cambridge University Press.

Wellman, P., & Tingey, R. J. (1981). Glaciation, erosion and uplift over part of East Antarctica. *Nature*, *291*(5811), 142–144. https://doi.org/10.1038/291142a0

Wessel, P., Smith, W. H. F., Scharroo, R., Luis, J., & Wobbe, F. (2013). Generic Mapping Tools: Improved version released. *Eos, Transactions American Geophysical Union*, *94*(45), 409–410. https://doi.org/10.1002/2013EO450001

White, D. A. (2013). Cenozoic landscape and ice drainage evolution in the Lambert Glacier-Amery Ice Shelf system. *Geological Society, London, Special Publications*, *381*(1), 151–165. https://doi.org/10.1144/SP381.15

Whitehouse, P. L., Bentley, M. J., Milne, G. A., King, M. A., & Thomas, I. D. (2012). A new glacial isostatic adjustment model for Antarctica: Calibrated and tested using observations of relative sea-level change and present-day uplift rates. *Geophysical Journal International*, *190*(3), 1464–1482. https://doi.org/10.1111/j.1365-246X.2012.05557.x

Wilson, D. S., Jamieson, S. S. R., Barrett, P. J., Leitchenkov, G., Gohl, K., & Larter, R. D. (2012). Antarctic topography at the Eocene-Oligocene boundary. *Palaeogeography, Palaeoclimatology, Palaeoecology*, *335-336*, 24–34. https://doi.org/10.1016/j.palaeo.2011.05.028

Wilson, D. S., & Luyendyk, B. P. (2006). Bedrock platforms within the Ross Embayment, West Antarctica: Hypotheses for ice sheet history, wave erosion, Cenozoic extension, and thermal subsidence. *Geochemistry, Geophysics, Geosystems*, *7*, Q12011. https://doi.org/10.1029/2006GC001294

Young, D. A., Wright, A. P., Roberts, J. L., Warner, R. C., Young, N. W., Greenbaum, J. S., et al. (2011). A dynamic early East Antarctic Ice Sheet suggested by ice-covered fjord landscapes. *Nature*, *474*(7349), 72–75. https://doi.org/10.1038/nature10114

Zachos, J., Pagani, M., Sloan, L., Thomas, E., & Billups, K. (2001). Trends, rhythms, and aberrations in global climate 65 Ma to present. *Science*, *292*(5517), 686–693. https://doi.org/10.1126/science.1059412

View publication stats